



CALiMERO

IMPROVING BIO-BASED INDUSTRIES LIFE CYCLE SUSTAINABILITY

D2.2: Identification and implementation of appropriate modeling strategy

Due date of submission: 30/06/2024

Actual submission date: 26/06/2024



**Funded by
the European Union**

TABLE OF CONTENTS

Table of contents.....	2
List of figures	3
List of tables.....	3
List of acronyms	4
Project information.....	5
Deliverable details	6
1 Introduction	7
2 Woodworking sector (WS)	8
2.1 Case study WS1: Emissions from the hot-pressing process during the production of Laminated Strand Lumber (LSL) boards	8
2.1.1 Case study description	8
2.1.2 Data collection	9
2.1.3 Modeling and simulation approach.....	9
2.2 Case study WS2: Emissions from energy production of LSL board production and externally delivered wood materials	9
2.2.1 Case study description	9
2.2.2 Data collection	10
2.2.3 Modeling and simulation approach.....	10
3 Textile sector (TS).....	12
3.1 Case study TS1: M50 washing after desizing	12
3.1.1 Case study description	12
3.1.2 Data collection	13
3.1.3 Modeling and simulation approach.....	13
4 Pulp & Paper Sector (PP).....	14
4.1 Case study PP1: Alternative chemical recovery routes in a pulp mill	14
4.1.1 Case study description	14
4.1.2 Data collection	15
4.1.3 Modeling and simulation approach.....	15
5 Biochemical sector (BS).....	15
5.1 Case study BS1: Downstream processing of second-generation bioethanol.....	15
5.1.1 Case study description	15
5.1.2 Data collection	16
5.1.3 Modeling and simulation approach.....	16
5.2 Case study BS2: Bioethylene production from second generation bioethanol.....	17

5.2.1	Case study description	18
5.2.2	Data collection	18
5.2.3	Modeling and simulation approach.....	18
6	Conclusions.....	19
7	References	20
8	Appendix	22

LIST OF FIGURES

Figure 1	Methodology to implement the appropriate modeling strategy for all bio-based sectors case studies	7
Figure 2	Laminated Strand Lumber (LSL) board.	8
Figure 3	Aspen Plus Simulation Flowsheet for size reduction and drying section	11
Figure 4	Aspen Plus Simulation Flowsheet for combustion section.....	11
Figure 5	Aspen Plus Simulation Flowsheet for heat recovery and steam generation section	12
Figure 6	Scheme depicting the M50 washing process after desizing	13
Figure 7	Aspen Plus Simulation Flowsheet for M50 Washing after Woven Desizing Process.....	14
Figure 8	Flowchart of chemical recovery with alternative process routes.....	14
Figure 9	Chemical recovery model with alternative process paths	15
Figure 10	Scheme depicting the downstream process for bioethanol purification	16
Figure 11	AVEVA process flowsheet for the beer stripping section	17
Figure 12	AVEVA process flowsheet for the rectification section.....	17
Figure 13	Scheme depicting the ethylene process	18
Figure 14	AVEVA process flowsheet for ethylene process.....	19

LIST OF TABLES

Table 1	Data set used in the case study 1 for the woodworking sector (4).....	23
Table 2	Methanol emissions model and statistics.....	24
Table 3	Acetic acid emissions model and statistics	25
Table 4	LMWAs emissions model and statistics	26
Table 5	Components included in the simulation model of case study 2 for the woodworking sector	28
Table 6	Properties of Corn starch	29
Table 7	Components included in the simulation model of case study for textile sector	29

LIST OF ACRONYMS

electrolyte nonrandom two-liquid (e-NRTL)	18	polymeric methylene diisocyanate resin (pMDI)	8
Laminated Strand Lumber (LSL)	7	pressure-swing adsorption (PSA)	17
Low Molecular Weight Acids (LMWAs)	25	universal quasichemical (UNIQUEAC)	15
methyl diethanolamine (MDEA).....	17	volatile organic compounds (VOCs)	7

PROJECT INFORMATION

Project full title: Industry CAse Studies AnaLysis To IMprove EnviRONmental Performance And Sustainability Of Bio-Based Industrial Processes

Acronym: CALIMERO

Call: HORIZON-CL6-2021-ZEROPOLLUTION-01

Topic: HORIZON-CL6-2021-ZEROPOLLUTION-01-06 - Increasing the environmental performance of industrial processes in bio-based sectors: construction, woodworking, textiles, pulp and paper and bio-chemicals

Start date: 1st July 2022

Duration: 48 months

List of participants:

Partner No.	PARTICIPANT ORGANIZATION ACRONYM
1 (Coord.)	Contactica CTA
2	WeLOOP WELOOP
3	European Cellulose Insulation Association ECIA
4	Swedish Environmental Research Institute IVL
5	Neovili NEOVILI
6	Cesefor CESEFOR
7	Luxembourg Institute of Science and Technology LIST
8	Technical University of Denmark DTU
9	Techtera TECHTERA
10	Essity ESSITY
11	BIM Kemi AB BIMKEMI
12	Ereks garment EREKS

DELIVERABLE DETAILS

Document Number:	D2.2
Document Title:	Identification and implementation of appropriate modeling strategy
Dissemination level	PU – Public
Period:	PR1 / PR2
WP:	WP2
Task:	T2.2
Author:	Gürkan Sin, Merlin Alvarado-Morales, Håkan Fridén, and Linnea Nilsson
Abstract:	This report presents the results of the development of appropriate simulation methods and the identification of the most relevant step in the value chain of the case studies. The formulation of appropriate models to simulate the current process and the proposed improvements is hereby described. This deliverable is related to T2.2.

Version	Date	Description
0	24 th June 2024	First draft of D2.2
1	25 th June 2024	Final version of D2.2

1 INTRODUCTION

CALIMERO (1) project is focused on improving the environmental performance of five bio-based sectors: construction, woodworking, textiles, pulp & paper, and biochemicals by developing a common framework working with PEF (Product Environmental Footprint) indicators as well as with those proposed by CALIMERO. An important building block of this framework is the development of appropriate mathematical models -to estimate material and energy flows as well as emissions through the different manufacturing stages of a specific product -and simulation strategies (model implementation) -matching the current process performance. Thus, modeling and simulation can serve a dual purpose in assessing sustainability improvements as well as further identification of process conditions and/or process parameters, process configurations that can reduce the carbon footprint, energy consumption, resource consumption, etc. The methodology outlined in Figure 1 has been followed to develop appropriate models and simulation strategies that match the model objectives defined in stage 1 for each bio-based sector case study.

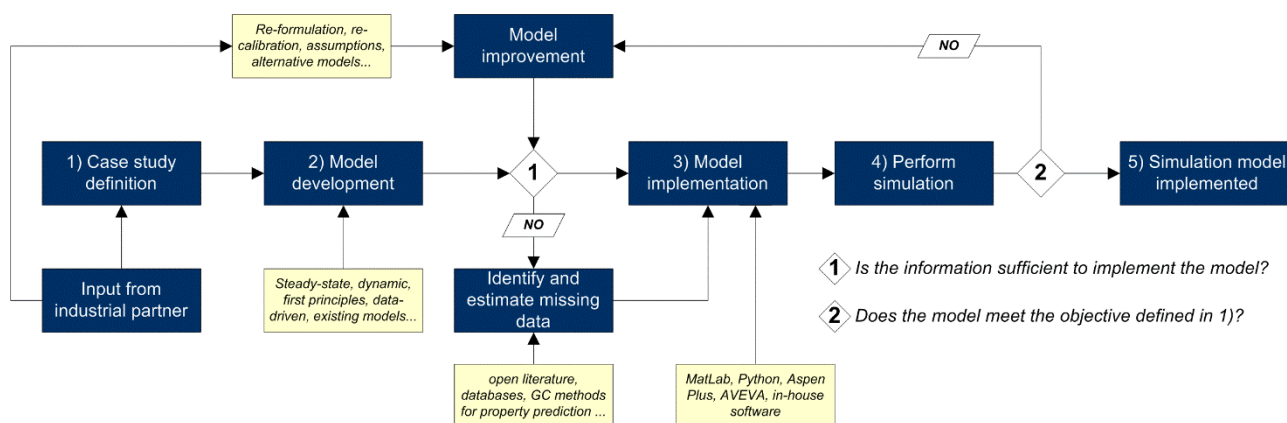


Figure 1 Methodology to implement the appropriate modeling strategy for all bio-based sectors case studies

Industrial partners were asked to provide information for each bio-based sector's case studies using a shared Excel spreadsheet created in stage 1 of the methodology. This served to define the model's objective and collect information such as process description, existing data, required data, modeling approach, existing simulation tools, and simulation strategies. The following sections comprise a description of the case study(s) that have been defined so far, data collection (both from industrial partners and open literature), model development, model implementation, and the simulation strategy applied for each case study.

2 WOODWORKING SECTOR (WS)

2.1 Case study WS1: Emissions from the hot-pressing process during the production of Laminated Strand Lumber (LSL) boards

2.1.1 Case study description

This case study is provided by the industrial partner Tabsal SCL S.L.¹, through CESEFOR. Tabsal manufactures structural wood composite products, such as Laminated Strand Lumber (LSL) board (Figure 2). LSL boards are manufactured from mainly poplar wood, which is converted into strands that are dried and bonded with a specific adhesive. Once oriented and stacked, these are introduced into a hydraulic press that applies heat (steam injection) and pressure to manufacture a board with a homogeneous density profile (2). The raw wood must be chopped into strands, and dried before blending with the adhesive². After pressing, the boards generally are cooled before stacking. The LSL panels are sanded and trimmed to the final dimensions, any other finishing operations (including laminate or veneer application) are done, and the finished product is packaged for shipment. These operations generated remnants that are blended with raw wood to be used as feedstock to a combustion process for energy recovery (case study 2).



Figure 2 Laminated Strand Lumber (LSL) board.

Emissions from hot pressing process are dependent on the type and amount of adhesive used to bind the wood strands together, wood species, wood moisture content, and press conditions (temperature and pressing time). When the press opens, vapors that may include adhesive ingredients and other volatile organic compounds (VOCs) are released. Emissions linked to the adhesive depend on the formulation of the adhesive while common VOC emissions comprise aldehydes, methanol, terpenes, and organic acids (3). Press temperature and time vary according to the molded product being produced but generally, total pressing time ranges from 2.5 min for a single opening press up to 6 min for multi-opening presses whilst press temperature can range from 130 to 288 °C³. Thus, our goal is to develop a mathematical model that predicts emissions resulting from the hot-pressing processing step based on operational conditions.

¹ <https://tabsal.com/en/home/>

² Personal communication with CESEFOR

³ <https://gaftp.epa.gov/ap42/ch10/s062/c10s06-2.pdf>

2.1.2 Data collection

Data provided by Tabsal via CESEFOR

The reference unit is m³ of the product since the board unit can have variability in its dimensions. The adhesive used in the LSL board production is a polyurethane-based resin known commercially as DESMODUR 1520 A20. The amount of adhesive used per m³ of a manufactured LSL board is around 35 kg. For 1 m³ of Lignumstrand, the average ratio would be 2 tons of green wood and 35 kg of adhesive. In the case of dry wood, we can calculate that of the 2 tons of round wood, approximately 700 kg of dry and screened chips will come out ready for the manufacture of the board. Emissions measurements as a function of the operating conditions of the press process were not available.

Data collected from open literature

Our first approach to data collection was to retrieve direct emissions measurements as a function of the hot-pressing conditions from open literature. For this, we have used the data set published by Jiang et al. (4)(Table 1 in the Appendix). The study investigated the effects of the different types of adhesive and pressing conditions on the VOC emissions released from hot-pressing mixed-hardwood particle boards. One of the adhesives assessed in this study is the polymeric methylene diisocyanate resin (pMDI), which Tabsal uses to produce LSL boards. However, only measured VOCs emissions were reported in this study, but not for the adhesive. Due to the lack of measurements in the open literature relating pressing conditions to adhesive emissions, an evaporation rate model proposed by the Center for the Polyurethanes Industry has been used to estimate adhesive emissions⁴. The description of this model can be found in the Appendix section.

2.1.3 Modeling and simulation approach

As the first iteration in our modeling strategy, a set of data-driven models was generated with the data sets reported by Jiang et al. Each model relates a set of input variables or predictors (pressing temperature, pressing time, resin content, moisture content, and board density) with an output variable, the emission of interest. Due to the value of some of the predictors being on a much larger scale than others including the output variable, the predictors were properly scaled (see *Equation 1* in Appendix). The MATLAB regression learner app has been used to generate the models. The models generated along with their corresponding statistics are shown in Table 2, Table 3, and Table 4 in the Appendix. The evaporation rate model used for the prediction of adhesive emissions considers operational conditions such as press time and temperature, adhesive content in the board as well as the composition of the adhesive (see Appendix). Lastly, these models were implemented in an Excel spreadsheet.

2.2 Case study WS2: Emissions from energy production of LSL board production and externally delivered wood materials

2.2.1 Case study description

This case study, provided by Tabsal SCL S.L., focuses on the emissions generated by the combustion of solid remnants from LSL production to produce energy. Solid remnants from board production and externally delivered wood materials are used to generate steam for drying and press operations⁵. As for the externally

⁴ Center for the Polyurethanes Industry, May 2012. MDI Emissions Reporting Guidelines for the Polyurethane Industry

⁵ Personal communication with CESEFOR

Funded by the European Union. Views and opinions expressed are however those of the author(s) only and do not necessarily reflect those of the European Union or European Research Executive Agency. Neither the European Union nor the granting authority can be held responsible for them.

delivered wood materials, these only include sawdust⁶.

2.2.2 Data collection

Data provided by Tabsal via CESEFOR

The feedstock to the combustion unit consists of 1000 kg of sawdust and 800 kg of solid remnants. The composition of solid remnants is dry wood splinters with the adhesive, there are no more raw materials in the product, and the press does not add anything other than steam for the glue to act, in the mentioned proportion.

Data collected from open literature

According to the BAT Reference Document (BREF) (5) the most important emissions to air from the combustion of solid fuels, such as biomass or wood residues, are SO_x, NO_x, CO, particulate matter (dust), and greenhouse gases such as CO₂. During the combustion of diisocyanate-based resin adhesive, emissions generated primarily contain CO₂ and CO. Smaller amounts of NO_x, hydrogen cyanide (HCN), and diisocyanate may also be present. The concentration and relative proportions of these gases depend mainly upon the combustion conditions and fuel composition (solid remnants and sawdust composition) (6). As a first approach, the combustion of solid remnants emits SO₂, NO, NO₂, CO, CO₂, N₂O, CH₄, HCN, HCL, and MDI. As for the wood composition (proximate, ultimate, and sulfanal analysis), namely, poplar wood and pine sawdust, these were retrieved from the ECN Phyllis classification database⁷. MDI properties were retrieved from NIST⁸ and CAMEO⁹ databases.

2.2.3 Modeling and simulation approach

Based on the information provided by the industrial partner and that collected from open literature, a simulation model was developed in ASPEN Plus for steady-state simulation. The compounds included in the simulation model are listed in Table 5 in the Appendix. The advantage of defining BIOMASS as a nonconventional component is that we can input attributes such as proximate, ultimate, and sulfanal analysis, retrieved from the ECN Phyllis classification database. The IDEAL property method (Ideal gas and Raoult's Law) has been used for the simulation model, since the process involves the conventional components such as H₂O, N₂, O₂, CO₂, etc., at low pressures. The implemented simulation model consists of three sections, namely, 1) size reduction and drying, 2) combustion, and 3) heat recovery and steam generation.

Section 1 – Size reduction and drying

The factory receives 2000 kg of poplar wood that is chopped and screened. A fraction of these (722 kg) is sent to the drier where part of the moisture is removed to attain a moisture content of 4.0% (w/w) resulting in 700 kg of chopped and dried wood. The unit operation models RStoic and Flash simulate a single piece of equipment for drying the wood. A calculator block is implemented to control the moisture content in the dried wood. The remaining fraction is sent to the combustion section.

⁶ Personal communication with CESEFOR

⁷ <https://phyllis.nl/Biomass/View/152>

⁸ <https://webbook.nist.gov/cgi/cbook.cgi?ID=101-68-8&Units=SI>

⁹ <https://cameochemicals.noaa.gov/chemical/8999>

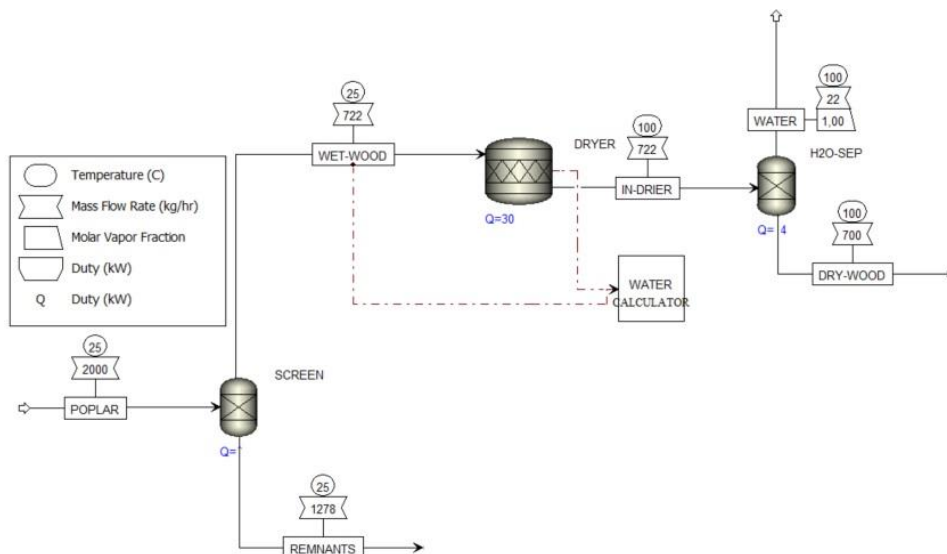


Figure 3 Aspen Plus Simulation Flowsheet for size reduction and drying section

Section 2 – Combustion

This section receives three streams, namely, 1000 kg of sawdust, the solid remnants from chopped and screened steps, and the remnants from the board production. It is considered that only 20 kg of these remnants are fed to the combustor with an adhesive composition of 4.7% (w/w). Thus, the amount of remnants from chopped and screened steps is adjusted to 780 kg so that the total adds up to 1800 kg of solid remnants sent to the combustion unit. A RGibbs model is used to simulate the combustion of the wood remnants. RGibbs models chemical equilibrium by minimizing the Gibbs free energy. However, the Gibbs free energy of wood remnants cannot be calculated because it is a nonconventional component defined in the simulation. Thus, before feeding the wood remnants to the RGibbs reactor model, the wood remnants must be decomposed into their constitute elements. This is done in the RYield block, DECOMP. The heat of reaction associated with the decomposition of wood remnants must be considered in the combustion of the wood remnants. Hence, a heat stream is used to carry this heat of reaction from the RYield reactor to the RGibbs reactor. Finally, the combustion gases are separated from the ashes using an SSPLIT model.

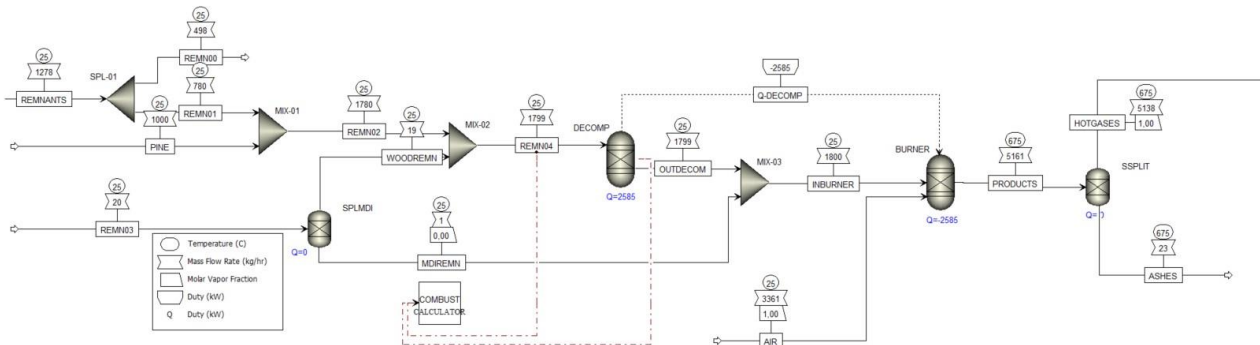


Figure 4 Aspen Plus Simulation Flowsheet for combustion section

Section 3 – Heat recovery and steam generation

Funded by the European Union. Views and opinions expressed are however those of the author(s) only and do not necessarily reflect those of the European Union or European Research Executive Agency. Neither the European Union nor the granting authority can be held responsible for them.

In this section, the heat from the combustion gases is recovered and used to produce steam. A heat stream is used to carry the heat of the combustion gases from the heat exchanger HEX01 to the heat exchanger HEX02. Fresh water is fed in HEX02 and heated up with the heat from HEX01 to generate steam. This steam can be used to cover some of the energy needs of the process.

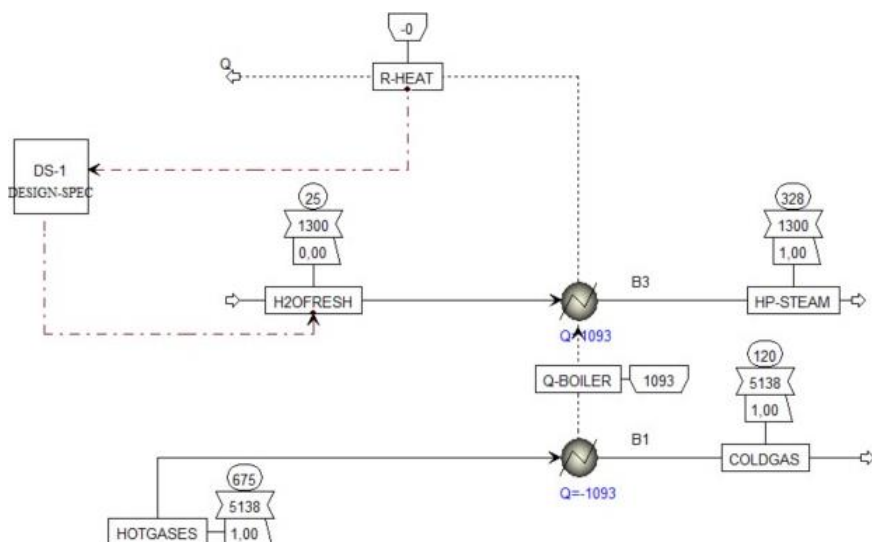


Figure 5 Aspen Plus Simulation Flowsheet for heat recovery and steam generation section

3 TEXTILE SECTOR (TS)

3.1 Case study TS1: M50 washing after desizing

3.1.1 Case study description

This case study is provided by the industrial partner TIL via TECHTERA and focuses on quantifying the amount of energy used in the M50 washing process while keeping a good level of cleanliness in the fabric. A scheme depicting the M50 process is shown in Figure 6. The woven impregnated with a sizing agent passes through a washing roller system comprising eight consecutive tanks (0 to 7). Clean cold water is fed to tanks 0-7 to wash the fabric and to a heat exchanger (HEX2) to cool down the dried woven fabric coming from the drier. Low-pressure (LP) steam is used to maintain the temperature inside the tanks (0-7) at 95 °C. After the washing process, the woven fabric passes through a roller dryer for moisture removal using LP steam. Once the moisture is removed, the fabric is cooled down with the HEX2 using clean cold water to recover heat from the hot fabric. The stream exiting (clean hot water) the HEX 2 is recycled back into tank 6. Part of the dirty hot water streams exiting tanks 0 and 7 are sent to the water treatment plant of the factory and the other fraction to the HEX1 to recover energy using a clean cold-water stream. The clean hot water stream exiting the HEX1 is recycled back into tanks 2 and 3 and the dirty cold water is sent to the wastewater treatment plant of the factory. To prevent overflow, a fraction of water is drained from each tank (1-6), and the rest is returned to the previous tank. The hot dirty water contains traces of the sizing agent removed from the fabric during the washing process.

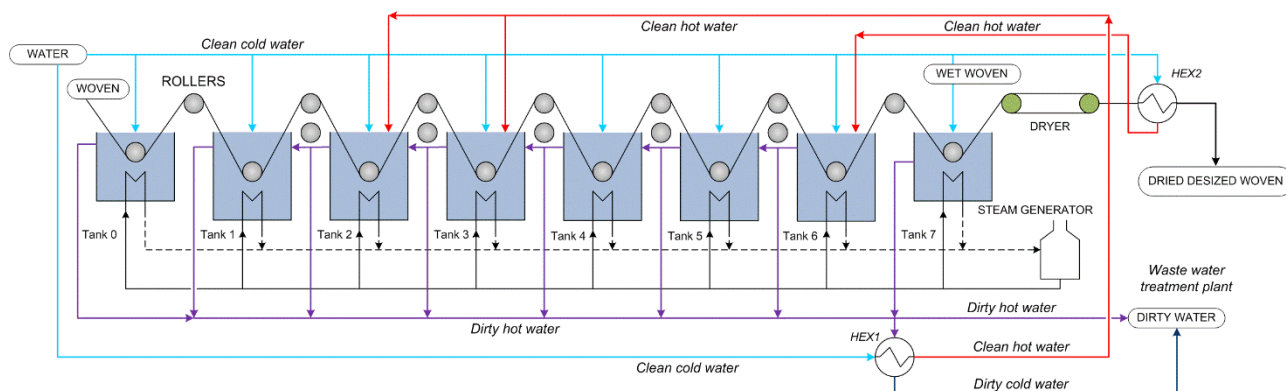


Figure 6 Scheme depicting the M50 washing process after desizing

Based on the process description and insights from the industrial partner, the objective is to develop a simulation model for the M50 washing process which can be used to investigate scenarios for energy recovery and further optimization purposes.

3.1.2 Data collection

Data provided by TIL via TECHTERA

Raw impregnated woven enters the process with a flow of 540 kg/h at ambient temperature. At steady state operation, the process runs with 5400 L/h of water. The tanks are supplied with clean cold water at a flow rate of 540 L/h and a temperature of 17°C, except for tank 6 which receives 1620 L/h. A steam circuit at 6 bar maintains the temperature in the tanks at 95 °C. Steam is produced in a boiler using natural gas as fuel. The sizing agent is completely removed during the washing process yielding a dried woven fabric with 0% of the sizing agent.

Data collected from open literature

Corn starch is chosen as the sizing material as it is one of the most common materials used as a textile sizing agent. This was later confirmed with the industrial partner when we visited TIL factory. The physicochemical properties of interest were taken from various sources (7–9). These properties, as summarized in Table 6 of the Appendix were essential for accurate modeling of starch behavior in aqueous solutions. Flory-Huggins model was used to model the solubility of starch in water. Flory Huggins interaction parameters for the starch-water system were collected from open literature (10). The molecular structure of corn starch was further elucidated by retrieving detailed information from the PubChem database, including a .mol file for precise molecular definition in Aspen Plus. This meticulous approach to characterizing corn starch was instrumental in the subsequent solubility analysis within the simulation framework.

3.1.3 Modeling and simulation approach

The compounds included in the simulation model are listed in Table 7 of the Appendix. Corn starch was defined as a user-defined biocomponent in the simulator. As already mentioned, the Flory-Huggins property method is set up for starch-water solubility calculations with the proper interaction parameters for the starch-water system (10). Based on the information provided by the industrial partner and that collected from open literature, a simulation model was developed in ASPEN Plus for steady-state simulation and the process flowsheet is shown in Figure 7. Three significant aspects driving the energy efficiency of the process that can be investigated with the simulation model are: (1) the split ratios, (2) the flowrates and temperatures of the recycled streams, and (3) the design specifications of HEX1 and HEX2.

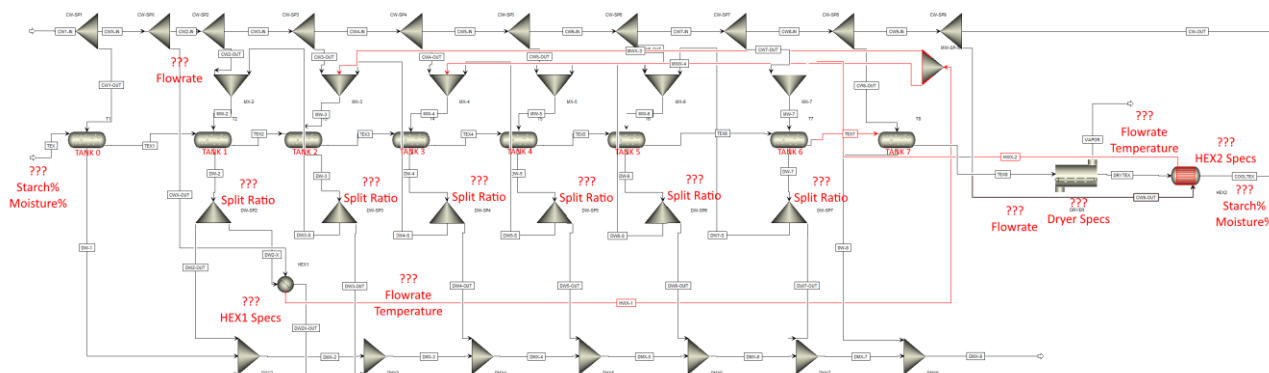


Figure 7 Aspen Plus Simulation Flowsheet for M50 Washing after Woven Desizing Process

4 PULP & PAPER SECTOR (PP)

4.1 Case study PP1: Alternative chemical recovery routes in a pulp mill

4.1.1 Case study description

This case study focuses on the environmental effect of alternative process routes in the chemical recovery of a pulp plant to reduce the PEF of produced tissue paper. The alternative process routes should not disturb the sodium/sulphur balance in the plant.

The alternative routes are:

- Lignin recovery (11) (12) (13) (14) to reduce recovery boiler load and thus increase production capacity.
- Electric plasma lime calcination (15) (16) to reduce bio and petrol fuel consumption.
- CO₂ capture (17) (18) from recovery boiler and calcination.

The chemical recovery section of the pulp plant is the focus of the simulation model as that is where the alternative process routes take place. A simplified flowchart of the pulp plant is presented in Figure 8. The alternative process routes are represented in green, the classical chemical recovery section is represented in purple, and the steps not part of the simulation are represented in orange.

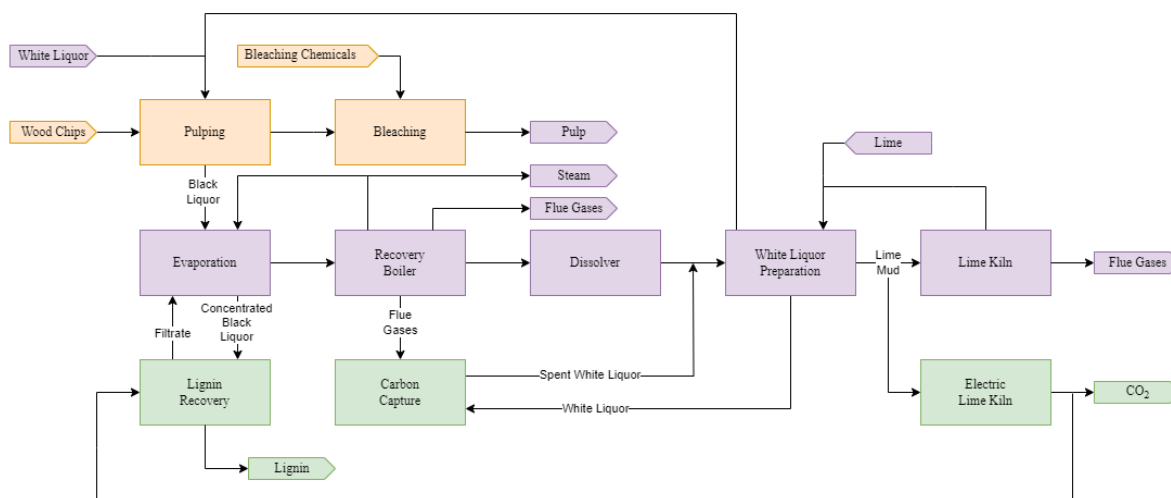


Figure 8 Flowchart of chemical recovery with alternative process routes

Funded by the European Union. Views and opinions expressed are however those of the author(s) only and do not necessarily reflect those of the European Union or European Research Executive Agency. Neither the European Union nor the granting authority can be held responsible for them.

4.1.2 Data collection

Data for model development and validation of the existing chemical recovery process and the alternative process routes are retrieved from the literature and non-disclosable mill. Additionally, the enthalpies of the solution used in the dissolver is retrieved from Zumdahl & Zumdahl (19), empirical constants for the causticizing reaction are presented by Ek et al. (20).

4.1.3 Modeling and simulation approach

A simulation model was developed in MatLab/Simulink for dynamic simulation as shown in Figure 9. The base model includes the pulp line, evaporator, recovery boiler, and the causticizer. The alternative process paths are lignin recovery (1), electric plasma lime calcination (6), and carbon capture using a white liquor scrubber (8).

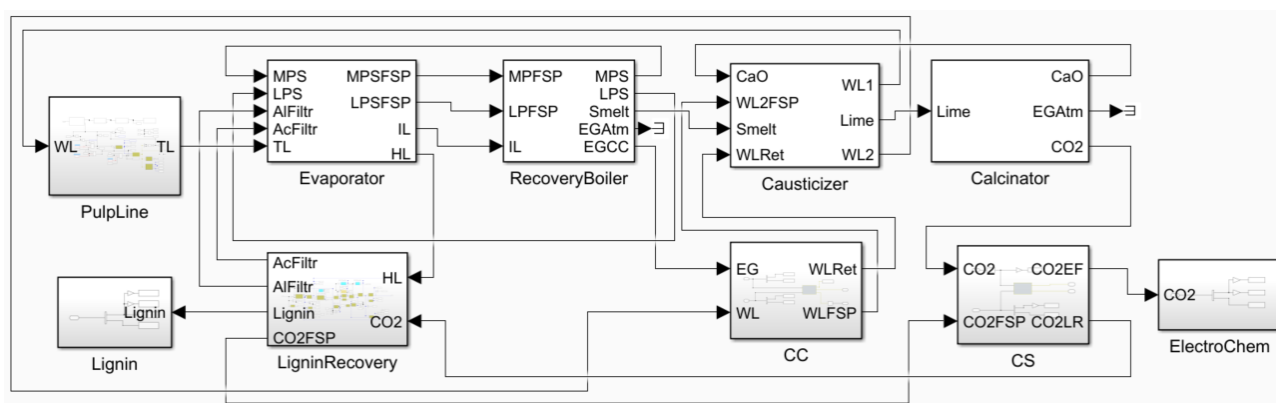


Figure 9 Chemical recovery model with alternative process paths

From the simulation, several properties can be obtained to be further used in the LCA study. These properties include chemicals consumption, flue gas emissions, net energy production (steam and electricity), captured CO₂ and produced pulp, tall oil, CNCG, and lignin.

In the simulation, the quantities of concentrated black liquor sent to lignin recovery, flue gases from the recovery boiler sent to carbon capture, and lime mud sent to an electric kiln can all be adjusted. This allows for the evaluation of the impact of the alternative process routes by examining the obtained properties mentioned above.

5 BIOCHEMICAL SECTOR (BS)

5.1 Case study BS1: Downstream processing of second-generation bioethanol

5.1.1 Case study description

This case study is provided by the industrial partner MELIORA via DTU and focuses on recovering bioethanol from the fermentation broth with an energy-efficient downstream process. The background scenario considered in this work is the second-generation bioethanol plant-wide simulation model developed by Prunescu et al. (21) for the MELIORA large-scale plant. The model includes pretreatment, enzymatic hydrolysis, and co-fermentation sections, respectively. The output of the plant-wide simulation model –the fermentation broth coming out from the co-fermentation section –is used as the input for the bioethanol downstream model developed for this case study. The proposed downstream process configuration (Figure 10) is based on

Funded by the European Union. Views and opinions expressed are however those of the author(s) only and do not necessarily reflect those of the European Union or European Research Executive Agency. Neither the European Union nor the granting authority can be held responsible for them.

Bisgaard et al. (22). In a first step, the beer stripper column separates the solids from the fermentation broth by stripping the product stream with steam. The remaining solids are separated from the beer column bottoms with a filter press and sent for combustion.

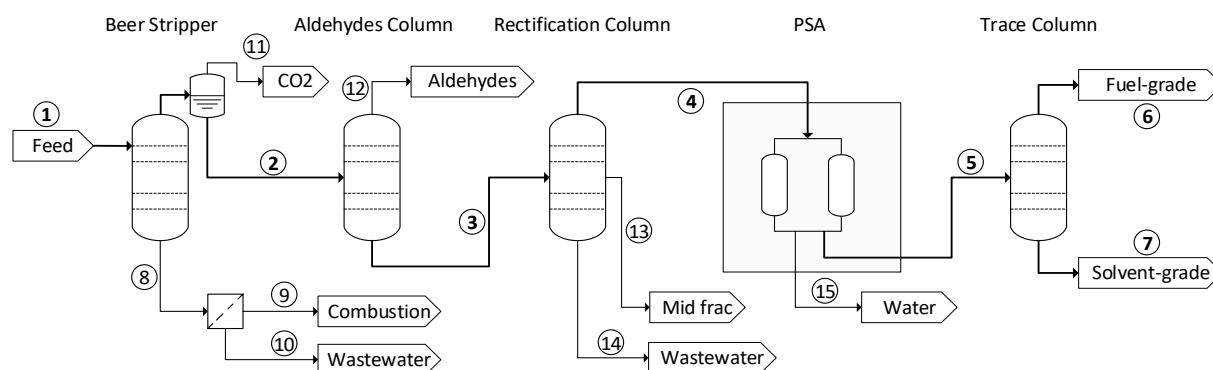


Figure 10 Scheme depicting the downstream process for bioethanol purification

The aldehydes column removes acetaldehyde, 1-propanal, 1-butanal, crotonaldehyde, and ethyl acetate. The main function of the third column, the rectification column, is to further concentrate ethanol up to a distillate with an azeotropic mixture of ethanol and water. The side draw is implemented to remove benzaldehyde, 1-propanol, 1-butanol, 2-butanol (s-butanol), 2-methyl-1-propanol, 2-methyl-1-butanol, and 3-methyl-1-butanol. The top product from the rectification column is sent to a molecular sieve unit to produce anhydrous ethanol. A fourth column, the trace column, is required to separate the remaining impurities, which are mainly methanol. Thereby, methanol can be separated with ethanol as the top product obtaining a solvent-grade ethanol with a purity of over 99.9 % (w/w) at the bottom.

5.1.2 Data collection

Data provided by MELIORA via DTU

The data for mass and energy balances as were retrieved from the plant-wide simulation model developed by Prunescu et al. (21). The simulation model has been validated using the data provided by MELIORA of their large-scale bioethanol plant.

Data collected from open literature

The data for mass and energy balances and operating conditions for the downstream separation were retrieved from Bisgaard et al. (22).

5.1.3 Modeling and simulation approach

Based on the information provided by the industrial partner and that collected from open literature, a simulation model was developed in AVEVA Simulator for steady-state simulation. The process flowsheet for the beer stripping and rectification sections is shown in Figure 11 and Figure 12. The impurities for detailed product grade analysis and the heat of combustion of solids have been included in the simulation model. Impurities were included using the same component-to-ethanol ratio as given in Bisgaard et al. (22). The inclusion of remaining solids after the fermentation was based on component property data from Wooley and Putsche (23). Vapor-liquid equilibrium is modeled with the activity-coefficient-based universal quasichemical (UNIQUAC) thermodynamic model and the interaction parameters data for component pairs are provided by AVEVA. The gas phase is modeled as an ideal gas, and the solubility of CO₂ is modeled using Henry's law. The initial configuration and equipment specifications were iteratively adapted using a Python-based sensitivity analysis

tool that offers an interface to AVEVA.

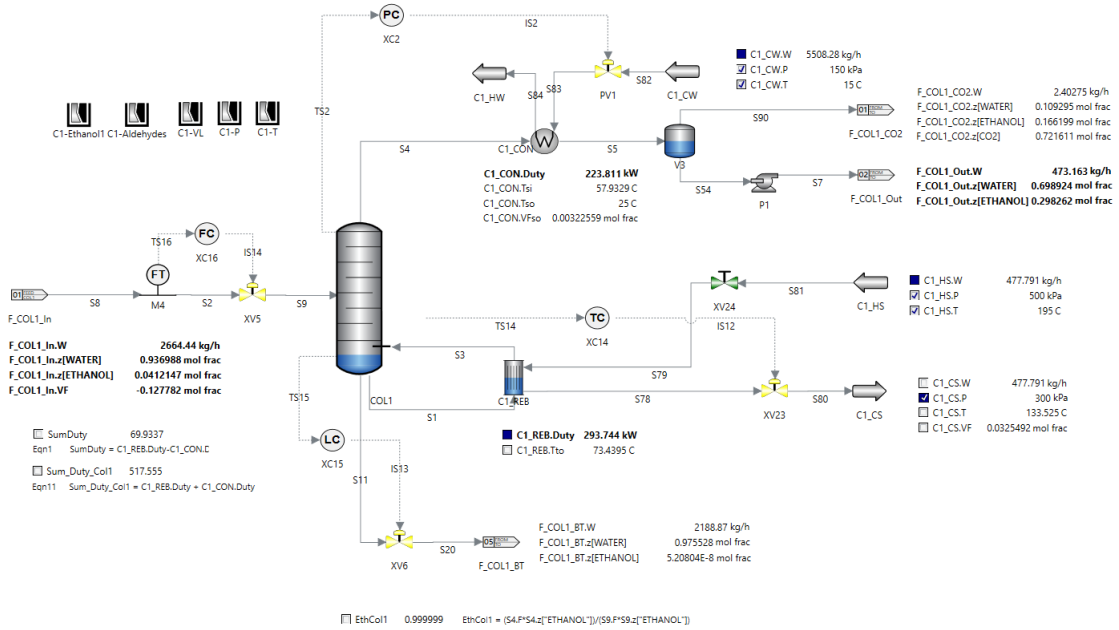


Figure 11 AVEVA process flowsheet for the beer stripping section

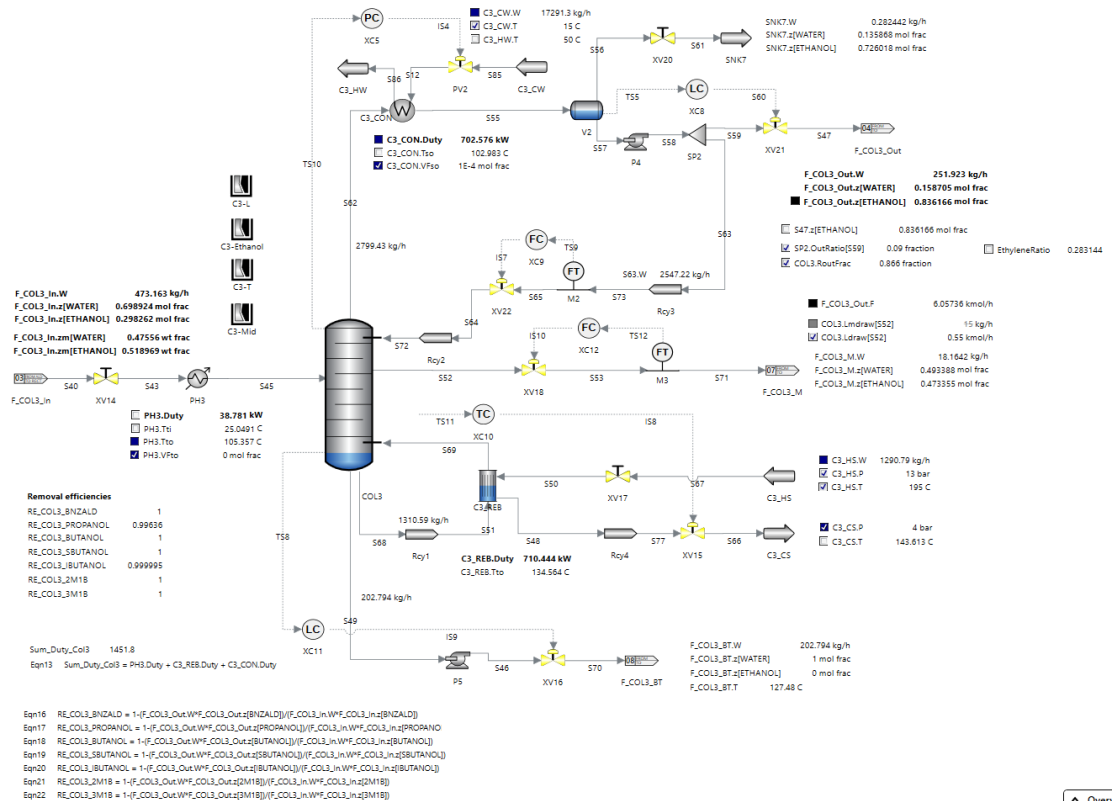


Figure 12 AVEVA process flowsheet for the rectification section

5.2 Case study BS2: Bioethylene production from second generation bioethanol

Funded by the European Union. Views and opinions expressed are however those of the author(s) only and do not necessarily reflect those of the European Union or European Research Executive Agency. Neither the European Union nor the granting authority can be held responsible for them.

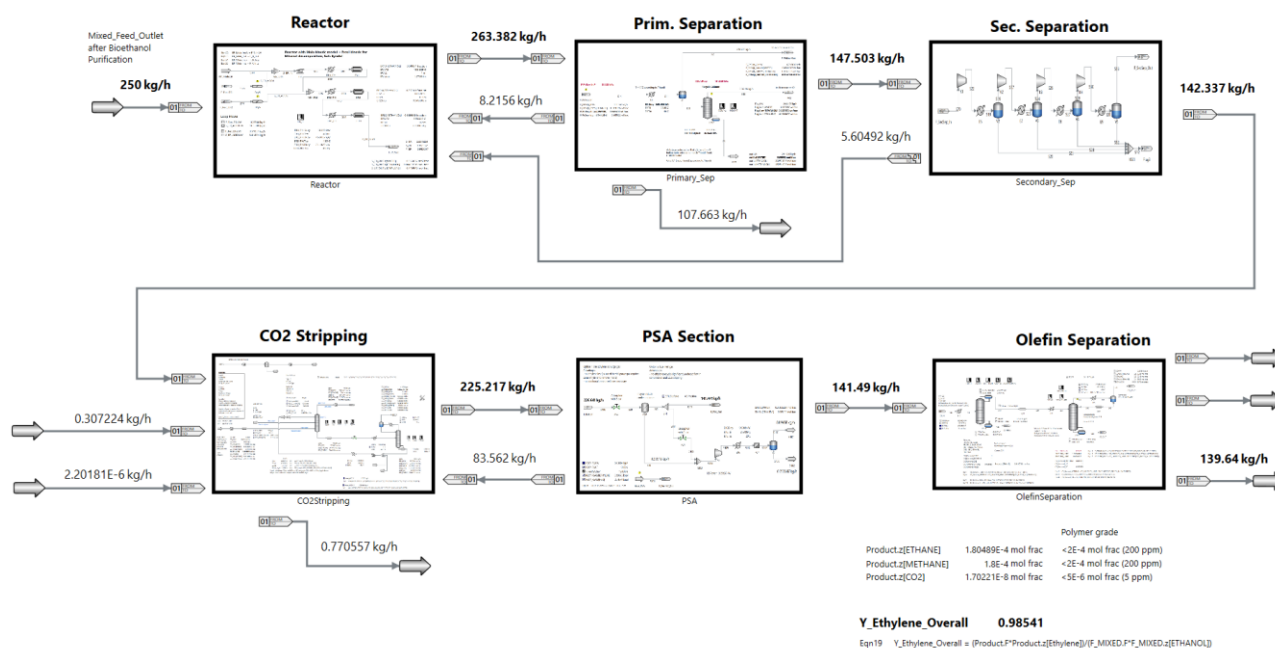


Figure 14 AVEVA process flowsheet for ethylene process

An adiabatic, fixed-bed plug-flow reactor with three sections was selected for ethanol dehydration. The reactor was modeled as a first principle model and implemented in MATLAB utilizing kinetic models from Maia et al. (25) and Tripodi et al. (27) of which both had plant/experimental data using a Syndol catalyst. After the reactor parameters were optimized, the model was transferred to AVEVA. In the CO₂-stripping section, electrolyte nonrandom two-liquid (e-NRTL) was used to correctly simulate the interactions between the charged species. The vapor-liquid equilibrium is based on an activity-coefficient model. The solubility of the light components CO, CO₂, O₂, N₂, H₂, CH₄, ethane, and propylene is modeled using Henry's law. The reactions taking place in the amine-based CO₂ absorption were implemented on all absorber stages, assuming equilibrium.

6 CONCLUSIONS

A set of simulation models for specific case studies from woodworking, textile, biochemical, and pulp and paper sectors has been developed. The models are based on insights from industrial CALIMERO partners as well as data retrieved from open literature. The models have been implemented in different simulation platforms such as AVEVA, Aspen, MatLab, and Simulink. In the following step, this model will be used to help partners with decision-making as well as to validate the proposed improvements that can reduce environmental footprint.

7 REFERENCES

1. <https://calimeroproject.eu/>.
2. <https://tabsal.com/en/the-product/> [Internet]. [cited 2023 Nov 27]. Available from: <https://tabsal.com/en/the-product/>
3. Centre JR, for Prospective Technological Studies I, Karlis P, Roudier S, Raunkjær Stubdrup K, Delgado Sancho L. Best available techniques (BAT) reference document for the production of wood-based panels – Industrial emissions Directive 2010/75/EU – Integrated pollution prevention and control. Publications Office; 2016.
4. Jiang T, Gardner DJ, Baumann MGD. Volatile organic compound emissions arising from the hot-pressing of mixed-hardwood particleboard. *For Prod J*. 2002;52(11–12):66–77.
5. Commission E, Centre JR, Neuwahl F, Brinkmann T, Lecomte T, Pinasseau A, et al. Best Available Techniques (BAT) reference document for large combustion plants – Industrial Emissions Directive 2010/75/EU (integrated pollution prevention and control). Publications Office; 2017.
6. Allport DC, Gilbert DS, Outterside SM, editors. MDI and TDI: Safety, Health and the Environment. Wiley; 2003.
7. Donovan JW, Mapes CJ. Multiple Phase Transitions of Starches and Nägeli Amylodextrins. *Starch - Stärke*. 1980 Jan 22;32(6):190–3.
8. Zhang L, Li G, Wang S, Yao W, Zhu F. Physicochemical properties of maca starch. *Food Chem*. 2017 Mar;218:56–63.
9. Kabo GJ, Voitkevich O V., Blokhin A V., Kohut S V., Stepurko EN, Paulechka YU. Thermodynamic properties of starch and glucose. *J Chem Thermodyn*. 2013 Apr;59:87–93.
10. Kumoro AC, Retnowati DS, Ratnawati R, Widiyanti M. Estimation of aqueous solubility of starch from various botanical sources using Flory Huggins theory approach. *Chem Eng Commun*. 2021 May 4;208(5):624–35.
11. Nilsson W. Lignin extraction from black liquor in a softwood pulping plant [Internet] [Master Thesis]. [Gothenburg, Sweden]: CHALMERS UNIVERSITY OF TECHNOLOGY; 2023 [cited 2024 Jun 24]. Available from: <https://odr.chalmers.se/items/5e540b47-5506-4708-a02b-98f4a0bbfa21>
12. Tomani P. Lignin Extraction from Black Liquor. In: In 43rd Pulp and Paper International Congress and Exhibition; Associacao Brasileira Tecnica de Celulose e Papel (ABTCP). Sao Paolo, Brazil; 2010.
13. Di Francesco D, Dahlstrand C, Löfstedt J, Orebom A, Verendel J, Carrick C, et al. Debottlenecking a Pulp Mill by Producing Biofuels from Black Liquor in Three Steps. *ChemSusChem*. 2021 Jun 8;14(11):2414–25.
14. Subramani A. Techno-Economic Assessment of a Post-Combustion CO₂ Capture Unit in SCA Östrand Pulp Mill [Internet] [Master Thesis]. [Stockholm, Sweden]: KTH Royal Institute of Technology; 2022 [cited 2024 Jun 24]. Available from: <https://kth.diva-portal.org/smash/record.jsf?pid=diva2%3A1685745&dsid=1521>
15. Erlandsson M, Holmström H, Karlsson PE, Mattson E, Neuwirth J, Nilsson Å. Underlagsdata för hållbarhetsbedömning i BioMapp – Arbetsrapport. IVL rapport C 572. 2024.
16. Andersson E, Skogström A. Process integration of electric plasma calcination in pulp and paper plants [Master Thesis]. [Gothenburg, Sweden]: Chalmers University of Technology; 2020.
17. Kuparinen K, Vakkilainen E, Tynjälä T. Biomass-based carbon capture and utilization in kraft pulp mills. *Mitig Adapt Strateg Glob Chang*. 2019 Oct 4;24(7):1213–30.
18. Cramstedt J. Carbon capture using white liquor in a Kraft pulping plant. Simulation and evaluation of a

Funded by the European Union. Views and opinions expressed are however those of the author(s) only and do not necessarily reflect those of the European Union or European Research Executive Agency. Neither the European Union nor the granting authority can be held responsible for them.

- scrubber [Master Thesis]. [Gothenburg, Sweden]: CHALMERS UNIVERSITY OF TECHNOLOGY; 2023.
19. Zumdahl SS, Zumdahl SA. Chapter 9.5: Enthalpies of Solution. In: Chemistry: An Atoms First Approach. 2011.
 20. Ek M, Gellerstedt G, Henriksson G. Pulp and Paper Chemistry and Technology. Vol. 2 Pulping Chemistry. 2016. 345–346 p.
 21. Prunescu RM, Blanke M, Jakobsen JG, Sin G. Model-based plantwide optimization of large scale lignocellulosic bioethanol plants. *Biochem Eng J.* 2017 Aug;124:13–25.
 22. Bisgaard T, Mauricio-Iglesias M, Huusom JK, Gernaey K V., Dohrup J, Petersen MA, et al. Adding Value to Bioethanol through a Purification Process Revamp. *Ind Eng Chem Res.* 2017 May 17;56(19):5692–704.
 23. Wooley RJ, Putsche V. Development of an ASPEN PLUS physical property database for biofuels components. Golden, CO; 1996 Apr.
 24. Frosi M, Tripodi A, Conte F, Ramis G, Mahinpey N, Rossetti I. Ethylene from renewable ethanol: Process optimization and economic feasibility assessment. *Journal of Industrial and Engineering Chemistry.* 2021 Dec;104:272–85.
 25. Maia JGSS, Demuner RB, Secchi AR, Melo PA, Carmo RW do, Gusmão GS. Process Modeling and Simulation of an Industrial-Scale Plant for Green Ethylene Production. *Ind Eng Chem Res.* 2018 May 9;57(18):6401–16.
 26. Mohsenzadeh A, Zamani A, Taherzadeh MJ. Bioethylene Production from Ethanol: A Review and Techno-economical Evaluation. *ChemBioEng Reviews.* 2017 Apr 31;4(2):75–91.
 27. Tripodi A, Belotti M, Rossetti I. Bioethylene Production: From Reaction Kinetics to Plant Design. *ACS Sustain Chem Eng.* 2019 Aug 5;7(15):13333–50.

8 APPENDIX

Woodworking sector

Table 1 Data set used in the case study 1 for the woodworking sector (4)

Exp	Press temp.	Press time	Resin content	Moisture content	Density	Formaldehyde	Methanol	Acetic acid	LMW acids (C1 - C4)	Hexanal	HMW VOCs
No.	°C	min	%	%	g/cm ³	mg/kg OD board					
1	182	5	3.5	13	0.77	0.31	2.70	23.60	24.00	12.70	29.70
2	199	3	2	12	0.71	0.07	4.80	12.00	13.40	31.70	69.00
3	165	7	2	14	0.83	0.16	13.10	39.30	40.70	29.70	73.90
4	165	3	2	14	0.71	0.09	2.60	2.80	2.90	12.60	26.20
5	165	7	5	14	0.71	0.35	8.20	26.20	27.60	19.10	43.20
6	199	3	5	14	0.71	0.10	2.10	10.90	11.20	13.40	30.20
7	199	7	2	14	0.71	0.34	9.70	37.30	42.60	14.00	34.60
8	165	3	5	12	0.71	0.09	1.70	4.90	5.10	9.80	21.10
9	165	7	5	12	0.83	0.20	7.90	29.10	29.40	22.60	54.40
10	182	5	3.5	13	0.77	0.23	6.60	28.50	30.50	18.90	46.00
11	165	3	5	14	0.83	0.03	0.90	2.50	2.80	12.60	26.60
12	165	7	2	12	0.71	0.15	10.40	30.20	31.40	28.60	67.00
13	199	7	5	12	0.71	0.90	9.60	48.00	55.70	15.50	43.80
14	199	7	5	14	0.83	0.85	5.40	44.40	52.20	11.30	36.10
15	199	3	5	12	0.83	0.09	3.10	12.10	12.80	17.00	36.90
16	165	3	2	12	0.83	0.02	0.80	0.80	0.90	6.10	15.50
17	199	3	2	14	0.83	0.16	5.60	13.80	14.10	19.70	47.00
18	199	7	2	12	0.83	0.51	15.50	50.80	57.70	29.70	81.80
19	182	5	3.5	13	0.77	0.33	6.00	26.40	28.30	5.00	25.30

Scaling predictor variables

$x_j^s = \frac{x_j - x_j^{min}}{x_j^{max}}$	<i>Equation 1</i>
x_j^s	scaled values of the predictor j
x_j	observed values of the predictor j
x_j^{min}	minimum value of the observed values of the predictor j
x_j^{max}	maximum value of the observed values of the predictor j

Data-driven models

Table 2 Methanol emissions model and statistics

Methanol emissions model						
	Coefficient	SE	tStat	pValue	+95%CI	-95%CI
β_0	2.501795	0.920710	2.717247	0.026361	0.378635	4.624955
β_1	9.165054	4.670757	1.962220	0.085365	-1.60573	19.93584
β_2	13.732002	1.450963	9.464058	0.000013	10.38607	17.07793
β_3	-5.152603	1.322671	-3.895605	0.004573	-8.20269	-2.10252
β_4	14.177304	5.289413	2.680317	0.027912	1.979895	26.37471
Predictors					min	max
x_1	Pressing temperature (°C)				165	199
x_2	Pressing time (min)				3	7
x_3	Resin content (% w/w)				2	5
x_4	Moisture content (% w/w)				12	14
x_5	Density of the board (g/cm ³)				0.71	0.83
Linear regression model w/o interactions:						
$y = \beta_0 + \beta_1 x_1 + \beta_2 x_2 + \beta_3 x_3 + \beta_4 x_5$						
RMSE	1.2374					
R-Squared Adjusted	0.8885					

Table 3 Acetic acid emissions model and statistics

Acetic acid emissions model

	Coefficient	SE	tStat	pValue	+95%CI	-95%CI
β_0	2.159868	1.736033	1.244140	0.231367	-1.520357	5.840093
β_1	68.406250	12.054300	5.674842	0.000034	42.852276	93.960224
β_2	53.703125	3.604175	14.900254	0.000000	46.062615	61.343635
Predictors					min	max
x_1	Pressing temperature (°C)				165	199
x_2	Pressing time (min)				3	7
x_3	Resin content (% w/w)				2	5
x_4	Moisture content (% w/w)				12	14
x_5	Density of the board (g/cm ³)				0.71	0.83
Linear regression model w/o interactions:						
$y = \beta_0 + \beta_1 x_1 + \beta_2 x_2$						
RMSE	4.1191					
R-Squared Adjusted	0.9334					

Table 4 LMWAs emissions model and statistics

Low Molecular Weight Acids (LMWAs) emissions model

	Coefficient	SE	tStat	pValue	+95%CI	-95%CI
β_0	-0.100000	0.215058	-0.464991	0.673610	-0.784411	0.584411
β_1	9.072059	1.275619	7.111888	0.005721	5.012470	13.131648
β_2	2.187500	0.391312	5.590170	0.011306	0.942171	3.432829
β_3	1.166667	0.131762	8.854377	0.003037	0.747343	1.585991
β_4	-21.700000	0.742462	-29.227080	0.000088	-24.062846	-19.337154
β_5	-0.691667	0.546811	-1.264911	0.295229	-2.431862	1.048528
β_6	44.043382	2.290326	19.230185	0.000307	36.754544	51.332220
β_7	17.150000	1.225000	14.000000	0.000789	13.251503	21.048497
β_8	14.583333	1.010363	14.433757	0.000721	11.367907	17.798759
β_9	-16.138889	1.152778	-14.000000	0.000789	-19.807542	-12.470236
β_{10}	99.254167	4.193006	23.671361	0.000165	85.910149	112.598184
Predictors					min	max
x_1	Pressing temperature (°C)				165	199
x_2	Pressing time (min)				3	7
x_3	Resin content (% w/w)				2	5
x_4	Moisture content (% w/w)				12	14
x_5	Density of the board (g/cm ³)				0.71	0.83
Linear regression model w/o interactions:						
	$y = \beta_0 + \beta_1x_1 + \beta_2x_2 + \beta_3x_3 + \beta_4x_4 + \beta_5x_5 + \dots$ $\beta_6x_1x_2 + \beta_7x_2x_4 + \beta_8x_3x_4 + \beta_9x_3x_5 + \beta_{10}x_4x_5$					
RMSE	0.0707					
R-Squared Adjusted	0.9994					

Evaporation rate model¹⁰¹¹

$E_{MDI} = \frac{\mathcal{M}\mathcal{W}_{MDI} k_{MDI} a p_{MDI}^{vap} \mathcal{K}_{MDI} C_{MDI}^f 3600 (1 - \% \eta_{filter}) \Theta F}{\mathcal{R} T}$	Equation 2	
$k_{MDI} = \frac{0.00438 \mathcal{U}^{0.78} \left(\frac{D_{MDI}}{3.1 \times 10^{-4}} \right)^{0.5}}{3.208}$	Equation 3	
$D_{MDI} = \frac{0.01013 T^{1.75} \left(\frac{1}{\mathcal{M}\mathcal{W}_{MDI}} + \frac{1}{\mathcal{M}\mathcal{W}_{air}} \right)^{0.5}}{P \left(\sum_j (\omega_j)^{1/3} \right)^2}$	Equation 4	
E_{MDI}	Evaporation rate	g/yr
$\mathcal{M}\mathcal{W}_{MDI}$	Molecular weight of MDI	g/mol
$\mathcal{M}\mathcal{W}_{air}$	Molecular weight of Air	g/mol
k_{MDI}	Gas mass transfer coefficient for MDI	m/s
a	Surface area exposed to air per unit (1 unit = 1 board)	m ² /unit
p_{MDI}^{vap}	Vapor pressure of MDI at temperature T	Pa
\mathcal{K}_{MDI}	Adjustment factor ¹²	-
C_{MDI}^f	Percentage of MDI/pDMI in the feed	%
\mathcal{R}	Ideal gas constant	m ³ Pa/K/mol
T	Temperature at which the pressing process takes place	K
\mathcal{U}	Air velocity over the product surface	m/s
D_{MDI}	Diffusion coefficient for MDI in air at a temperatura T ¹³	m ² /s
ω_j	GC values for MDI summed over atoms, groups, and structural features	-
P	Atmospheric pressure	Pa
η_{filter}	Filter efficiency	%
Θ	Pressing time – the time at which the product stays at an elevated temperature	h
F	Annual production	unit/yr

¹⁰ Methods for Estimating Air Emissions from Paint, Ink, and Other Coating Manufacturing Facilities, volume II: Chapter 8, 2005.

¹¹ Methods for Estimating Air Emissions from Chemical Manufacturing Facilities, volume II: Chapter 16, 2007.

¹² Check excel file for calculation of this parameter.

¹³ Fuller-Schettler-Giddings correlation (Table 5-10, Perry 8th Edition)

Table 5 Components included in the simulation model of case study 2 for the woodworking sector

Component ID	Type	Component name
H ₂	Conventional	Hydrogen
CH ₄	Conventional	Methane
CO	Conventional	Carbon monoxide
CO ₂	Conventional	Carbon dioxide
O ₂	Conventional	Oxygen
N ₂	Conventional	Nitrogen
NO	Conventional	Nitric oxide
NO ₂	Conventional	Nitrogen dioxide
SO ₂	Conventional	Sulfur dioxide
H ₂ O	Conventional	Water
HCl	Conventional	Hydrogen chloride
Cl ₂	Conventional	Chlorine
HCN	Conventional	Hydrogen cyanide
DIPHE-01	Conventional	Diphenylmethane-4,4-diisocyanate
DIPHE-02	Solid	Diphenylmethane-4,4-diisocyanate
BIOMASS	Nonconventional	Poplar wood, sawdust, wood remnants
ASH	Nonconventional	Ashes
C	Solid	Carbon
S	Conventional	Sulfur

Table 6 Properties of Corn starch

Starch (type)	T _{gel} (K)	H _{fus} (J/mol)	T _m (K)	MW (g/mol)	w _{ash} (%)
Corn	339.00	42300	460.2	1.80 x 10 ⁰⁸	0.23 ± 0.01

Table 7 Components included in the simulation model of case study for textile sector

Component ID	Type	Component name
H ₂ O	Conventional	Water
Starch	Biocomponent	Corn starch
ASH	Nonconventional	Ash